

Mathematical modeling

Математическое моделирование

UDC 629.78

<https://doi.org/10.32362/2500-316X-2023-11-6-47-56>



RESEARCH ARTICLE

Mathematical modeling of velocity and accelerations fields of image motion in the optical equipment of the Earth remote sensing satellite

Sergei Yu. Gorchakov [®]

MIREA – Russian Technological University, Moscow, 119454 Russia

[®] Corresponding author, e-mail: sygorchakov@yandex.ru

Abstract

Objectives. The paper considers a satellite with an optoelectronic payload designed to take pictures of the Earth's surface. The work sets out to develop a mathematical model for determining the dependencies between the state vector of the satellite, the state vector of the point being imaged on the Earth's surface, and the distribution fields of the velocity vectors and accelerations of the motion of the image along the focal plane of the optoelectronic payload.

Methods. The method is based on double differentiation of the photogrammetry equation when applied to a survey of the Earth's surface from space. For modeling the orbital and angular motion of the satellite, differential equations with numerical integration were used. The motion parameters of the Earth's surface were calculated based on the Standards of fundamental astronomy software library.

Results. Differential equations of motion of the image were obtained. Verification of the developed mathematical model was carried out. The motion of the considered satellite was simulated in orbital orientation mode using an image velocity compensation model. The distribution fields of velocity vectors and accelerations of motion of the image of the Earth's surface were constructed. The residual motion of the field of image following compensation was investigated.

Conclusions. The proposed mathematical model can be used both with an optoelectronic payload when modeling shooting modes and estimating image displacements at the design stage of a satellite, as well as at the satellite operation stage when incorporating the presented model in the onboard satellite software. The presented dependencies can also be used to construct an image transformation matrix, both when restoring an image and when obtaining a super-resolution.

Keywords: remote sensing of the Earth, satellite, images of Earth's landscapes, mathematical model, image velocity field, image acceleration field, super-resolution

• Submitted: 25.07.2022 • Revised: 04.05.2023 • Accepted: 07.09.2023

For citation: Gorchakov S.Yu. Mathematical modeling of velocity and accelerations fields of image motion in the optical equipment of the Earth remote sensing satellite. *Russ. Technol. J.* 2023;11(6):47–56. <https://doi.org/10.32362/2500-316X-2023-11-6-47-56>

Financial disclosure: The author has no a financial or property interest in any material or method mentioned.

The author declares no conflicts of interest.

НАУЧНАЯ СТАТЬЯ

Математическое моделирование полей скоростей и ускорений движения изображения в оптической аппаратуре спутника дистанционного зондирования Земли

С.Ю. Горчаков [®]

МИРЭА – Российский технологический университет, Москва, 119454 Россия

[®] Автор для переписки, e-mail: sygorchakov@yandex.ru

Резюме

Цели. В статье рассматривается спутник с оптико-электронной аппаратурой, предназначеннной для съемки поверхности Земли. Цель статьи – разработка математической модели для определения зависимостей между вектором состояния спутника, вектором состояния снимаемой точки на земной поверхности и полями распределений векторов скоростей и ускорений движения изображения по фокальной плоскости оптико-электронной аппаратуры.

Методы. Используемый метод основан на двойном дифференцировании уравнения фотограмметрии при применении его к съемке поверхности Земли из космоса. Для построения модели орбитального и углового движений спутника применяются дифференциальные уравнения с численным интегрированием. Параметры вращения Земли и движения земной поверхности вычисляются на основе библиотеки программ Standards of fundamental astronomy.

Результаты. Получены дифференциальные уравнения движения изображения. Проведена верификация разработанной математической модели. Проведено моделирование движения спутника в режиме орбитальной ориентации и в режиме компенсации скорости движения изображения. Построены поля распределения векторов скоростей и ускорений движения изображения поверхности Земли. Исследовано остаточное поле движения изображения после компенсации.

Выводы. Предложенная математическая модель может найти применение как на этапе проектирования спутника с оптико-электронной аппаратурой при моделировании режимов съемки и оценках смещений изображения, так и на этапе эксплуатации спутника при применении представленной модели в бортовом программном обеспечении спутника. Представленные зависимости также можно использовать для построения матрицы сдвига изображения в задачах восстановления изображения и получения сверхразрешения.

Ключевые слова: дистанционное зондирование Земли, спутник, изображения ландшафтов Земли, математическая модель, поле скоростей движения изображения, поле ускорений движения изображения, сверхразрешение

• Поступила: 25.07.2022 • Доработана: 04.05.2023 • Принята к опубликованию: 07.09.2023

Для цитирования: Горчаков С.Ю. Математическое моделирование полей скоростей и ускорений движения изображения в оптической аппаратуре спутника дистанционного зондирования Земли. *Russ. Technol. J.* 2023;11(6):47–56. <https://doi.org/10.32362/2500-316X-2023-11-6-47-56>

Прозрачность финансовой деятельности: Автор не имеет финансовой заинтересованности в представленных материалах или методах.

Автор заявляет об отсутствии конфликта интересов.

INTRODUCTION

The paper considers a satellite equipped with a high-resolution imaging optoelectronic payload (OEP) with charge-coupled photosensitive devices (CCPD) operating in a time delay and integration (TDI) mode. The TDI technology is based on multiple exposures of the same object, which significantly increases the signal-to-noise ratio and can thus be used for scanning low-light scenes, but imposes limitations on its application, since it becomes necessary to ensure the movement of the projected image of the object in accordance with the movement of charge packets on photodetectors.¹

The accuracy at which the image motion velocity (IMV) is known sharply limits the use of TDI technology. In order to ensure that the accumulated shift during the exposure time does not exceed $\sim 1/3$ of a pixel, it is necessary to account for such IMV vector fields on a CCPD [1].

Among the main components of the superposition of the charge packet motion along CCPD during the exposure time are the orbital and angular motion of the satellite, the curvature of the Earth's surface and its rotation, as well as operational errors of the satellite attitude control and stabilization system (ACSS).

Many authors have dealt with issues of IMV calculation. The calculation of IMV fields is considered in [2–4]. In [2, 3, and 5], problems associated with calculating the velocity field of image motion when a satellite moves in a central gravitational field are also considered.

Compensation of IMV fields is considered in [6–9]. These works discuss the method of providing the required (reference) IMV by means of a satellite's rotational motion in accordance with the special program law of orientation and stabilization control.²

The present author assumes that, in the presence of compensation, there may be deviations of actual IMV from the required value, for example, due to unauthorized

turns of the satellite due to errors in the ACSS operation, possible vibrations affecting the satellite structure, as well as scanning without considering terrain relief.

The present work aims to develop a general mathematical model for calculating IMV fields and image motion acceleration (IMA) vectors taking into account the main dynamic and kinematic factors of the imaging process, as well as to estimate the residual IMV and IMA fields in the presence of compensation. In the presented mathematical model of IMV calculation, unlike [2, 3, and 5], the main dynamic effects of external and internal forces and torques forcing on the satellite body may be taken into account.

The obtained results can be used in compiling an image field shift matrix for solving the super-resolution problem.

PROBLEM STATEMENT

We shall construct a mathematical model of scanning the Earth's surface from space based on the following assumptions:

1. The satellite model represents a completely solid body orbiting the Earth according to the EGM2008 gravitational field model [10].
2. The model of the onboard OEP represents a completely solid body with focal distance f and focal plane (FP) having dimensions a and b .
3. The Earth model is an ellipsoid with WGS84 parameters.³
4. Coordinate systems used: geocentric celestial inertial reference system (GCRS) [11]; international terrestrial reference system (ITRS) [11]; local-vertical-local-horizontal (LVLH) coordinate system or orbital frame (OF) [12]; satellite body frame (BF); and OEP focal plane frame (FPF). For writing down equations of the satellite motion, the inertial quasi-non-moving GCRS coordinate system is used. When writing differential equations of the satellite motion in the rotating ITRS coordinate system, it is necessary to consider the precession and nutation of the Earth in motion

¹ Hang Y. *Time-Delay-Integration CMOS Image Sensor Design for Space Applications*: Ph.D. Thesis. Nanyang Technological University; 2016.

² Galkina A.S. *Synthesis of the Spacecraft Angular Motion Control Programs for Surveying Curvilinear Routes*. Diss. ... Cand. Sci. (Eng.). Samara; 2011. 143 p. (in Russ.).

³ https://gssc.esa.int/navipedia/index.php/Reference_Frames_in_GNSS. Accessed August 23, 2023.

equations. Considering precession, nutation, and motion of the Earth's poles, as well as transition parameters between the International Atomic Time (TAI) and Coordinated Universal Time (UTC) scales are included in the corresponding matrices in the Earth rotation model using the software package provided by Standards of Fundamental Astronomy (SOFA) [13, 14].

5. The time scales used are TAI and UTC [11].

The following functional dependencies need to be defined:

$$\begin{aligned} \mathbf{v}_{x,y} &= \dot{\mathbf{x}}_{x,y} = f(\mathbf{r}_{\text{sat}}, \mathbf{v}_{\text{sat}}, \mathbf{q}_{\text{sat}}, \mathbf{w}_{\text{sat}}, \mathbf{r}_e, \mathbf{v}_e, \mathbf{a}_e); \\ \mathbf{a}_{x,y} &= \ddot{\mathbf{x}}_{x,y} = f(\mathbf{r}_{\text{sat}}, \mathbf{v}_{\text{sat}}, \dot{\mathbf{v}}_{\text{sat}}, \mathbf{q}_{\text{sat}}, \mathbf{w}_{\text{sat}}, \dot{\mathbf{w}}_{\text{sat}}, \mathbf{r}_e, \mathbf{v}_e, \mathbf{a}_e), \end{aligned} \quad (1)$$

where $\mathbf{v}_{x,y}$ is the vector of IMV at the point with x and y coordinates on the FP; $\mathbf{a}_{x,y}$ is the vector of IMA; $\mathbf{r}_{\text{sat}}, \mathbf{v}_{\text{sat}}, \dot{\mathbf{v}}_{\text{sat}}$ are position, velocity, and acceleration of the satellite in the GCRS, respectively; $\mathbf{q}_{\text{sat}}, \mathbf{w}_{\text{sat}}, \dot{\mathbf{w}}_{\text{sat}}$ are orientation quaternion, angular velocity, and angular acceleration of the satellite in the BF, respectively; $\mathbf{r}_e, \mathbf{v}_e, \mathbf{a}_e$ are position, velocity, and acceleration of the scanned point on the Earth's surface, respectively.

The schematic explaining the problem statement is shown in Fig. 1.

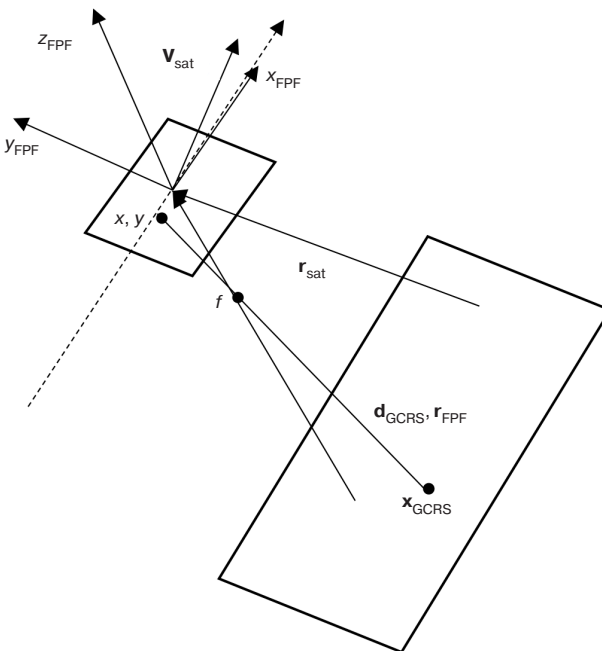


Fig. 1. Graphical representation of problem statement

MATHEMATICAL SURVEYING MODEL

According to the fundamental equation of space photogrammetry, the relationship between the FPF and the GCRS with respect to scale (in image space)

is defined using a system of collinearity equations [15] expressed in projections on the FPF axis, as follows:

$$x = fXZ^{-1}; y = fYZ^{-1}, \quad (2)$$

where x, y are the coordinates of the image point in the FPF (in image space).

We define the range vector \mathbf{r}_{FPF} expressed in the FPF coordinate system (in object space), using the following relationship:

$$\mathbf{r}_{\text{FPF}} = \mathbf{M}_{\text{GCRS}}^{\text{FPF}} \mathbf{d}_{\text{GCRS}}, \quad (3)$$

where \mathbf{d}_{GCRS} is the scanning range vector in the GCRS connecting the point on the FPF and the point to be imaged on the Earth's surface; $\mathbf{M}_{\text{GCRS}}^{\text{FPF}} = \mathbf{M}_{\text{BF}}^{\text{FPF}} \mathbf{M}_{\text{GCRS}}^{\text{BF}}$ is conversion matrix from the GCRS to the FPF; $\mathbf{M}_{\text{BF}}^{\text{FPF}}$ is conversion matrix from the BF to the FPF; $\mathbf{M}_{\text{GCRS}}^{\text{BF}}$ is conversion matrix from the GCRS to the BF (satellite orientation matrix).

Equations (2) and (3) describe the process when the imaging object and FP are stationary; x, y coordinates, \mathbf{d}_{GCRS} vector, and $\mathbf{M}_{\text{GCRS}}^{\text{FPF}}$ matrix are unchanged. Since scanning of the Earth's surface from space takes place over time, all components in the above equations are functions of time.

MATHEMATICAL MODEL FOR IMAGE MOTION VELOCITY

In order to find the IMV vector at the point FP, we differentiate Eqs. (2) by time, as follows:

$$\begin{aligned} \dot{x} &= \frac{d}{dt} fXZ^{-1} + f \frac{d}{dt} (XZ^{-1}); \\ \dot{y} &= \frac{d}{dt} fYZ^{-1} + f \frac{d}{dt} (YZ^{-1}), \end{aligned}$$

The first summand $\frac{d}{dt} fXZ^{-1} = 0$, since the focal length is a constant value within the framework of the problem to be solved. Then:

$$\begin{aligned} \dot{x} &= f \frac{d}{dt} (XZ^{-1}) = f \frac{V_x Z - X V_z}{Z^2} = \\ &= (fV_x - xV_z) Z^{-1}; \\ \dot{y} &= f \frac{d}{dt} (YZ^{-1}) = f \frac{V_y Z - Y V_z}{Z^2} = \\ &= (fV_y - yV_z) Z^{-1}, \end{aligned} \quad (4)$$

where $V_x = \frac{d}{dt} X$ и $V_y = \frac{d}{dt} Y$.

For defining vector $\mathbf{v}_{\text{FPF}} = \{O_{\text{FPF}}, V_x, V_y, V_z\}$, we differentiate Eq. (3), as follows:

$$\begin{aligned} \mathbf{v}_{\text{FPF}} &= \frac{d}{dt} \mathbf{r}_{\text{FPF}} = \frac{d}{dt} \mathbf{M}_{\text{GCRS}}^{\text{FPF}} \mathbf{d}_{\text{GCRS}} + \\ &+ \mathbf{M}_{\text{GCRS}}^{\text{FPF}} \frac{d}{dt} \mathbf{d}_{\text{GCRS}}. \end{aligned} \quad (5)$$

We define the derivative of the transformation matrix $\mathbf{M}_{\text{GCRS}}^{\text{FPF}}$, as follows:

$$\frac{d}{dt} \mathbf{M}_{\text{GCRS}}^{\text{FPF}} = \frac{d}{dt} \mathbf{M}_{\text{BF}}^{\text{FPF}} \mathbf{M}_{\text{GCRS}}^{\text{BF}} + \mathbf{M}_{\text{BF}}^{\text{FPF}} \frac{d}{dt} \mathbf{M}_{\text{GCRS}}^{\text{BF}}.$$

In the resulting equation, since there is no rotation between FPF and BF (FP and satellite structure) according to the problem statement conditions, the first summand reverses to zero.

Then after substituting Poisson's equation $\frac{d}{dt} \mathbf{M}_{\text{GCRS}}^{\text{FPF}} = -\mathbf{W}_x \mathbf{M}_{\text{GCRS}}^{\text{FPF}}$ [5], we obtain from (5) the following:

$$\begin{aligned} \mathbf{v}_{\text{FPF}} &= \mathbf{M}_{\text{GCRS}}^{\text{FPF}} \frac{d}{dt} \mathbf{d}_{\text{GCRS}} - \\ &- \mathbf{M}_{\text{BF}}^{\text{FPF}} \mathbf{W}_x \mathbf{M}_{\text{GCRS}}^{\text{BF}} \mathbf{d}_{\text{GCRS}}, \end{aligned} \quad (6)$$

where $\mathbf{W}_x = [\mathbf{\omega} \times] = \begin{bmatrix} 0 & -\omega_z & \omega_y \\ \omega_z & 0 & -\omega_x \\ -\omega_y & \omega_x & 0 \end{bmatrix}$ is the angular velocity matrix of the satellite in BF.

Equation (6) shows that the total IMV is composed of translational and angular motions of the OEP and the imaging object.

We proceed to finding functional dependencies for the IMA.

MATHEMATICAL MODEL FOR IMAGE MOTION ACCELERATION

For determining the IMA, we differentiate Eq. (4) for the second time, as follows:

$$\begin{aligned} \ddot{x} &= \frac{d}{dt} \left(f(V_x Z - X V_z) Z^{-2} \right) = \\ &= f \left[(A_x Z - X A_z) Z^{-2} - 2V_z (V_x Z - X V_z) Z^{-3} \right]; \\ \ddot{y} &= \frac{d}{dt} \left(f(V_y Z - Y V_z) Z^{-2} \right) = \\ &= f \left[(A_y Z - Y A_z) Z^{-2} - 2V_z (V_y Z - Y V_z) Z^{-3} \right]. \end{aligned} \quad (7)$$

For determining acceleration vector $\mathbf{a}_{\text{FPF}} = \{O_{\text{FPF}}, A_x, A_y, A_z\}$ in the FPF, we differentiate Eq. (5) for the second time, as follows:

$$\begin{aligned} \mathbf{a}_{\text{FPF}} &= \frac{d}{dt} \left[\frac{d}{dt} \mathbf{M}_{\text{GCRS}}^{\text{FPF}} \mathbf{d}_{\text{GCRS}} + \mathbf{M}_{\text{GCRS}}^{\text{FPF}} \frac{d}{dt} \mathbf{d}_{\text{GCRS}} \right] = \\ &= \frac{d^2}{dt^2} \mathbf{M}_{\text{GCRS}}^{\text{FPF}} \mathbf{d}_{\text{GCRS}} + 2 \frac{d}{dt} \mathbf{M}_{\text{GCRS}}^{\text{FPF}} \frac{d}{dt} \mathbf{d}_{\text{GCRS}} + \mathbf{M}_{\text{GCRS}}^{\text{FPF}} \frac{d^2}{dt^2} \mathbf{d}_{\text{GCRS}}. \end{aligned} \quad (8)$$

We rewrite Eq. (8) in the following form:

$$\begin{aligned} \mathbf{a}_{\text{FPF}} &= -\frac{d}{dt} \left[\mathbf{M}_{\text{BF}}^{\text{FPF}} \mathbf{W}_x \mathbf{M}_{\text{GCRS}}^{\text{BF}} \right] \mathbf{d}_{\text{GCRS}} - \\ &- 2 \mathbf{M}_{\text{BF}}^{\text{FPF}} \mathbf{W}_x \mathbf{M}_{\text{GCRS}}^{\text{BF}} \frac{d}{dt} \mathbf{d}_{\text{GCRS}} + \\ &+ \mathbf{M}_{\text{BF}}^{\text{FPF}} \mathbf{M}_{\text{GCRS}}^{\text{BF}} \frac{d^2}{dt^2} \mathbf{d}_{\text{GCRS}}; \\ \mathbf{a}_{\text{FPF}} &= - \left\{ \underbrace{\left[\frac{d}{dt} \mathbf{M}_{\text{BF}}^{\text{FPF}} \mathbf{W}_x \mathbf{M}_{\text{GCRS}}^{\text{BF}} + \right]}_0 + \mathbf{M}_{\text{BF}}^{\text{FPF}} \frac{d}{dt} \mathbf{W}_x \mathbf{M}_{\text{GCRS}}^{\text{BF}} + \right. \\ &\left. + \mathbf{M}_{\text{BF}}^{\text{FPF}} \mathbf{W}_x \frac{d}{dt} \mathbf{M}_{\text{GCRS}}^{\text{BF}} \right] \mathbf{d}_{\text{GCRS}} \right\} - \\ &- 2 \mathbf{M}_{\text{BF}}^{\text{FPF}} \mathbf{W}_x \mathbf{M}_{\text{GCRS}}^{\text{BF}} \frac{d}{dt} \mathbf{d}_{\text{GCRS}} + \\ &+ \mathbf{M}_{\text{BF}}^{\text{FPF}} \mathbf{M}_{\text{GCRS}}^{\text{BF}} \frac{d^2}{dt^2} \mathbf{d}_{\text{GCRS}}; \\ \mathbf{a}_{\text{FPF}} &= \mathbf{M}_{\text{BF}}^{\text{FPF}} \left[-\mathbf{E}_x \mathbf{M}_{\text{GCRS}}^{\text{BF}} \mathbf{d}_{\text{GCRS}} - \right. \\ &- \mathbf{W}_x \mathbf{W}_x \mathbf{M}_{\text{GCRS}}^{\text{BF}} \mathbf{d}_{\text{GCRS}} - \\ &- 2 \mathbf{W}_x \mathbf{M}_{\text{GCRS}}^{\text{BF}} \frac{d}{dt} \mathbf{d}_{\text{GCRS}} + \\ &\left. + \mathbf{M}_{\text{GCRS}}^{\text{BF}} \frac{d^2}{dt^2} \mathbf{d}_{\text{GCRS}} \right], \end{aligned} \quad (9)$$

where $\mathbf{E}_x = [\mathbf{e} \times] = \begin{bmatrix} 0 & -e_z & e_y \\ e_z & 0 & -e_x \\ -e_y & e_x & 0 \end{bmatrix}$ is the angular acceleration matrix of the satellite in the BF.

In the resulting equation, the first summand is the Euler acceleration, the second summand is the centripetal acceleration, while the third summand is the Coriolis acceleration. Next, we define the range vector \mathbf{d}_{GCRS} and its derivatives.

MATHEMATICAL MODEL FOR THE POINT MOTION ON THE EARTH'S SURFACE

Equations of the point motion on the Earth's surface are written as follows:

$$\begin{aligned} \mathbf{x}_{\text{GCRS}} &= \mathbf{M}_{\text{ITRS}}^{\text{GCRS}} \mathbf{x}_{\text{ITRS}}; \\ \dot{\mathbf{x}}_{\text{GCRS}} &= \mathbf{M}_{\text{ITRS}}^{\text{GCRS}} \dot{\mathbf{x}}_{\text{ITRS}} + \boldsymbol{\omega}_{\text{GCRS}} \times \mathbf{x}_{\text{GCRS}}; \\ \ddot{\mathbf{x}}_{\text{GCRS}} &= \mathbf{M}_{\text{ITRS}}^{\text{GCRS}} \ddot{\mathbf{x}}_{\text{ITRS}} - \boldsymbol{\omega}_{\text{GCRS}} \times \\ &\quad \times (\boldsymbol{\omega}_{\text{GCRS}} \times \mathbf{x}_{\text{GCRS}}) + 2\boldsymbol{\omega}_{\text{GCRS}} \times \\ &\quad \times \dot{\mathbf{x}}_{\text{GCRS}} + \dot{\boldsymbol{\omega}}_{\text{GCRS}} \times \mathbf{x}_{\text{GCRS}}, \end{aligned} \quad (10)$$

where \mathbf{x}_{ITRS} , $\dot{\mathbf{x}}_{\text{ITRS}}$, $\ddot{\mathbf{x}}_{\text{ITRS}}$ are position, velocity, and acceleration of the point on the Earth's surface (in the ITRS), respectively; $\mathbf{M}_{\text{ITRS}}^{\text{GCRS}}$ is the rotation matrix between the ITRS and GCRS coordinate systems; $\boldsymbol{\omega}_{\text{GCRS}}$ is the angular velocity vector of the Earth's rotation in the GCRS.

The angular acceleration vector of the Earth rotation can be neglected ($\dot{\boldsymbol{\omega}}_{\text{GCRS}} \approx 0$).

Then the range, relative velocity, and relative acceleration vectors can be defined as follows:

$$\begin{aligned} \mathbf{d}_{\text{GCRS}} &= \mathbf{x}_{\text{GCRS}} - \mathbf{x}_{\text{sat}} = \mathbf{M}_{\text{ITRS}}^{\text{GCRS}} \mathbf{x}_{\text{ITRS}} - \mathbf{x}_{\text{sat}}; \\ \dot{\mathbf{d}}_{\text{GCRS}} &= \dot{\mathbf{x}}_{\text{GCRS}} - \dot{\mathbf{x}}_{\text{sat}} = \mathbf{M}_{\text{ITRS}}^{\text{GCRS}} \dot{\mathbf{x}}_{\text{ITRS}} + \\ &\quad + \boldsymbol{\omega}_{\text{GCRS}} \mathbf{x}_{\text{GCRS}} - \dot{\mathbf{x}}_{\text{sat}}; \\ \ddot{\mathbf{d}}_{\text{GCRS}} &= \ddot{\mathbf{x}}_{\text{GCRS}} - \ddot{\mathbf{x}}_{\text{sat}} = \\ &= \mathbf{M}_{\text{ITRS}}^{\text{GCRS}} \ddot{\mathbf{x}}_{\text{ITRS}} - \boldsymbol{\omega}_{\text{GCRS}} \times (\boldsymbol{\omega}_{\text{GCRS}} \times \mathbf{x}_{\text{GCRS}}) + \\ &\quad + 2\boldsymbol{\omega}_{\text{GCRS}} \times \dot{\mathbf{x}}_{\text{GCRS}} - \ddot{\mathbf{x}}_{\text{sat}}. \end{aligned} \quad (11)$$

The vector field of velocities and accelerations along the FP are obtained by substituting the resulting Eqs. (11) into (9) and (6), calculating the IMV and IMA vectors in accordance with Eqs. (4) and (7) at each point of FP.

VERIFICATION

We compare the results obtained in the presented mathematical model with those obtained in [2] for the same initial data.

Based on calculations using the proposed mathematical model at the point with coordinates $(0, 0)$, the following IMV values are obtained: 46.951 mm/s along the x axis and 2.592 mm/s along the y axis. In [2], values of 46.921 mm/s in the x axis and 2.591 mm/s in the y axis are obtained. Thus, the calculation relative error is no more than 0.1%, which indicates the reliability of the proposed model for calculating the IMV.

Table 1. Initial data for modeling

Parameter	Unit of measure (UoM)	Numerical value
Satellite inclination	degree	60.000
Orbit eccentricity	—	0.01
Semi-major axis of the orbit	km	6678.000
OEP focus distance, f	m	1.500
FP dimensions	mm	120 × 80

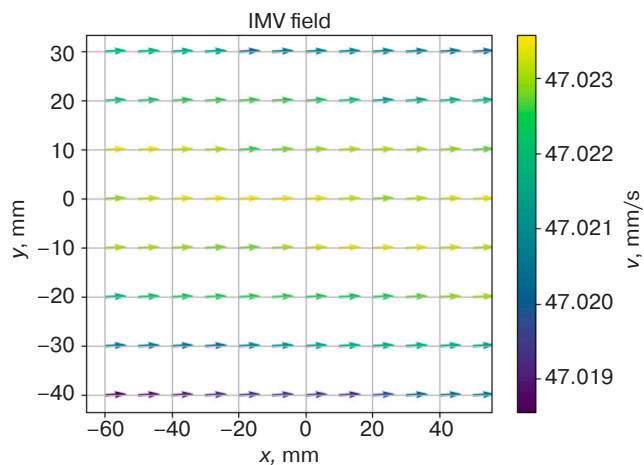


Fig. 2. Verification of the model

MODELING

The program is developed based on the mathematical model. The satellite dynamics are described by differential equations of the solid body motion [7, 12]. The satellite state vector is integrated using the fourth order Runge–Kutta method [12] in the TAI time scale [11]. In the linear perturbation part of the satellite motion, only the acceleration due to the effects of the Earth's gravitational field with a 20×20 decomposition according to the EGM2008 model [10] is considered, while in the angular perturbation part, only the control torques determined using a proportional derivative controller based on the mismatch between the actual angular motion and the reference motion are taken into account. When calculating the transition matrix from GCRS to ITRS and calculating the transition between TAI and UTC time scales, the program library provided by SOFA [14] is used.

Two cases are considered. In the first case, the satellite is in orbital orientation (the BF axes are co-directed with the LVLH axes), while in the second case, the satellite rotation parameters correspond to the reference angular motion at which the IMV compensation is provided [7].

Modeling is carried out for the three sets of initial data presented in Tables 2–4.

Table 2. Initial data for modeling

Parameter	UoM	Numerical value
Modeling start time	UTC	2020-01-01 00:00:00.000000
Modeling end time	UTC	2020-01-01 00:30:00.000000
Satellite inclination	degree	97.000
Orbit eccentricity	–	0.001
Semi-major axis of the orbit	km	6900.000
OEP focus distance, f	m	2.000
FP dimensions	mm	160 × 20
Reference IMV in the FP center	mm/s	20.000
Reference IMV at the FP right edge	mm/s	20.000

The results of the field modeling without compensation are shown in Figs. 3 and 4.

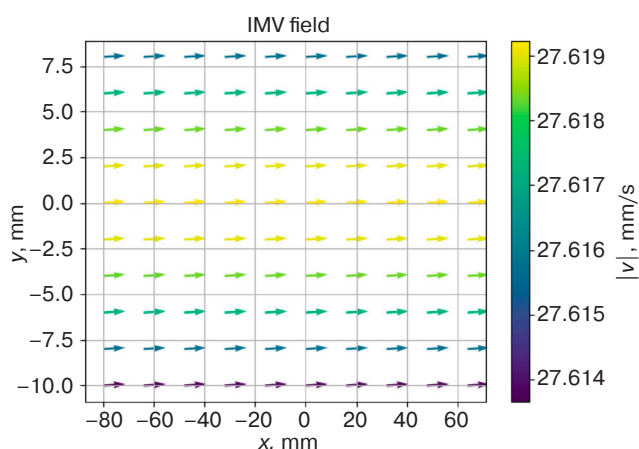


Fig. 3. Field of IMV vectors without compensation

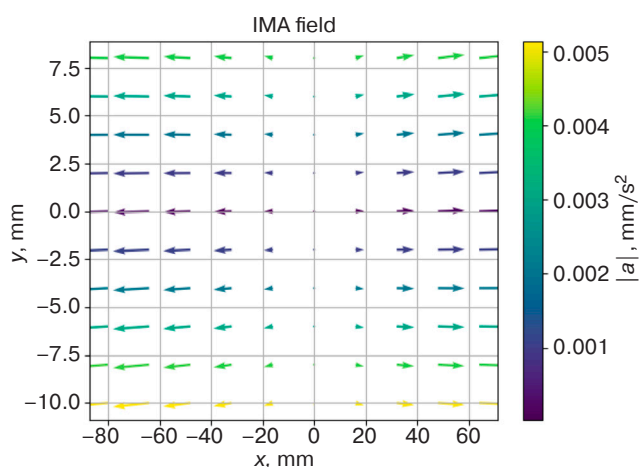


Fig. 4. Field of IMA vectors without compensation

The modeling results of the residual IMV and IMA fields with compensation (reference IMV along $x = 20$ mm/s, along $y = 0$ mm/s) are shown in Figs. 5 and 6.

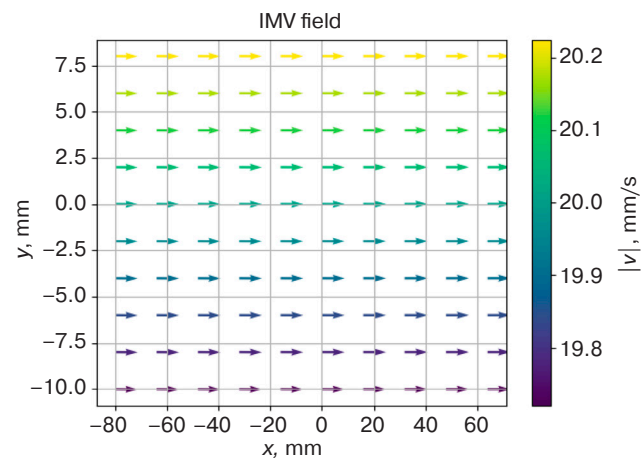


Fig. 5. Field of IMV vectors with compensation

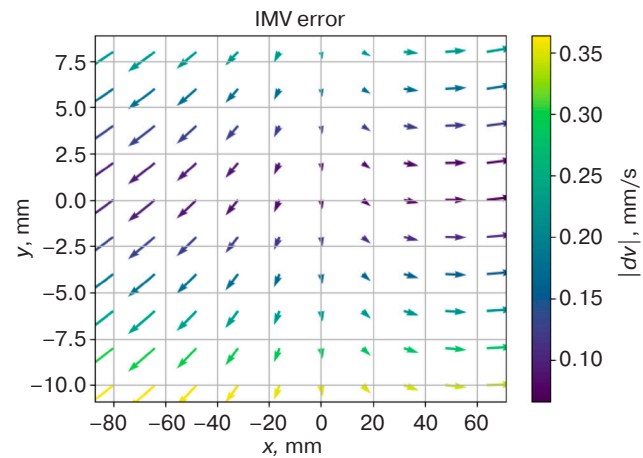


Fig. 6. Difference between the reference and actual fields of the IMV after compensation

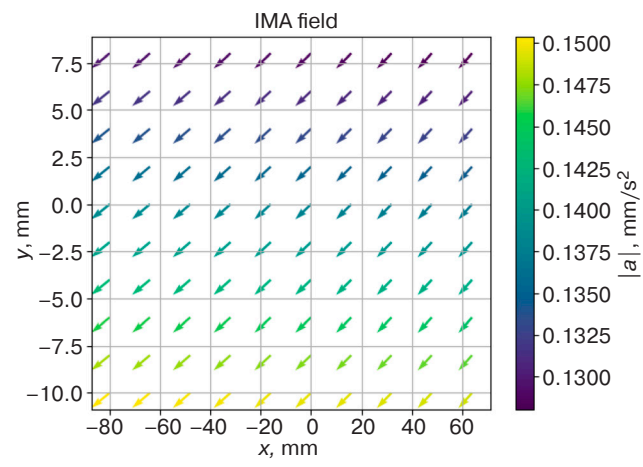


Fig. 7. Field of IMA vectors with compensation

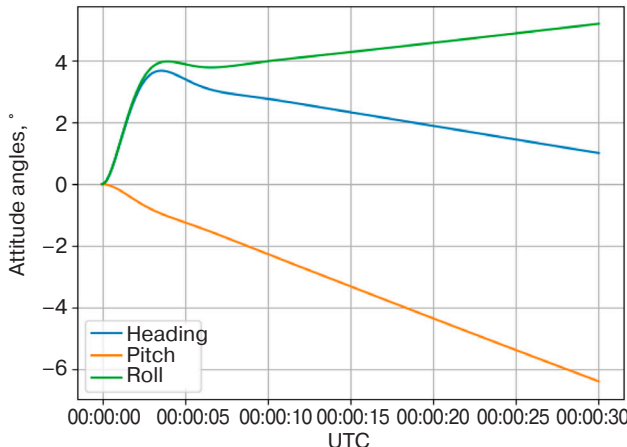


Fig. 8. Satellite attitude angles relative to LVLH

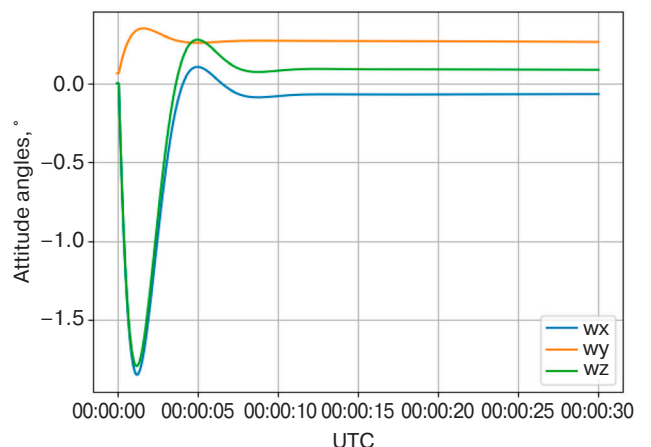


Fig. 9. Satellite angular rates relative to BF

The residual transverse velocity field of IMV (along the y -axis) can be seen in Fig. 6. This may be explained by the fact that when calculating the reference angular velocity using the algorithm described in [7], two points are taken as reference points: in the center of FP and at the right edge of FP (in the considered case, corresponding to the coordinates $[0, 10]$). It is at these points that the actual IMV is equal to the reference IMV.

Thus, the modeling shows that the residual field exists even when the compensation algorithm is used, allowing such coordinates of the FP to be selected in which the IMV reference vector is required.

The graphs of satellite attitude angles and satellite angular velocities in the IMV compensation mode are presented in Figs. 8 and 9.

The fields of IMV and IMA vectors without compensation are presented in Figs. 10 and 11.

Table 3. Initial data for modeling

Parameter	UoM	Numerical value
Modeling start time	UTC	2020-01-01 00:00:00.000000
Modeling end time	UTC	2020-01-01 00:30:00.000000
Satellite inclination	degree	97.000
Orbit eccentricity	—	0.001
Semi-major axis of the orbit	km	7000.000
OEP focus distance, f	m	2.000
FP dimensions	mm	160 × 20

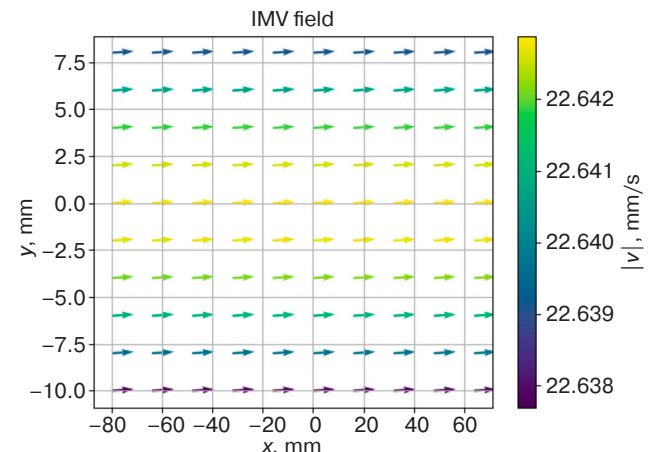


Fig. 10. Field of IMV vectors without compensation

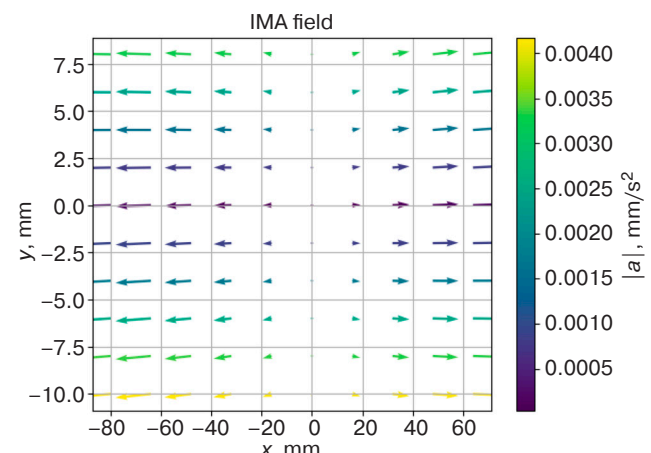


Fig. 11. Field of IMA vectors without compensation

Figure 12 shows the field of IMV with compensation. Figure 13 indicates the difference between the reference and actual fields of IMV after compensation.

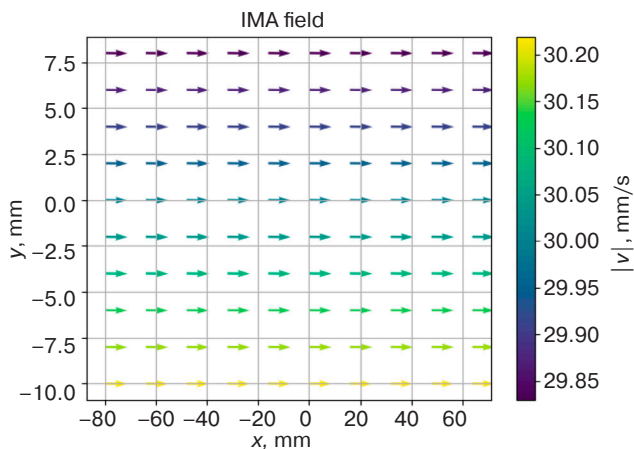


Fig. 12. Field of IMV vectors with compensation

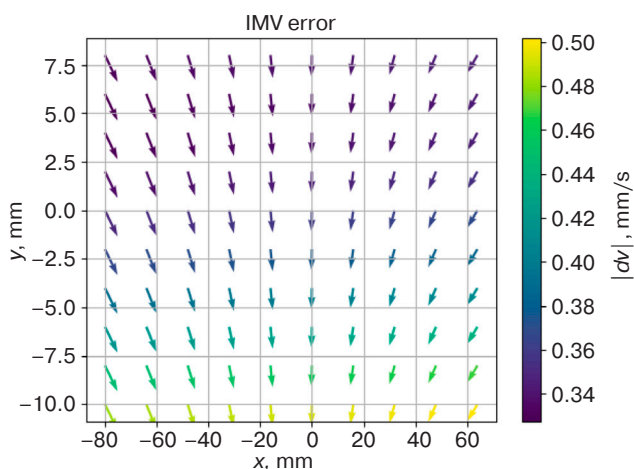


Fig. 13. Difference between the reference and actual fields of IMV after compensation

Table 4. Initial data for modeling

Parameter	UoM	Numerical value
Modeling start time	UTC	2020-01-01 00:00:00.000000
Modeling end time	UTC	2020-01-01 00:30:00.000000
Satellite inclination	degree	97.000
Orbit eccentricity	—	0.001
Semi-major axis of the orbit	km	7000.000
OEP focus distance, f	m	2.000
FP dimensions	mm	160 × 20
Reference IMV in the FP center	mm/s	30.000
Reference IMV at the FP right edge	mm/s	30.000

CONCLUSIONS

The obtained and presented mathematical dependencies can be used for calculating the vector fields of image motion velocities and accelerations on photodetectors of the optoelectronic payloads installed on the satellite.

The dependencies can also be used to estimate the accumulated image displacement during the exposure time at the ground stage and preventing shooting with inappropriate image motion velocities during satellite operation, i.e., preventing directional “blurring” of the image. As a result, they may find application in calculating the image shift matrix for super-resolution.

REFERENCES

1. Gecha V.Ya., Zhilenev M.Yu., Gorchakov S.Yu., Novoselov S.A. Formulas for calculating the kinematic parameters of the planet's orbital survey by the spacecraft's on-board optic imager when taking into account the required the velocity of the image motion on its photodetector. *Voprosy elektromekhaniki. Trudy VNIEM = Electromechanical Matters. VNIEM Studies.* 2019;173(6):23–32 (in Russ.). Available from URL: <https://jurnal.vniem.ru/text/173/23-32.pdf>
2. Gecha V.Y., Zhilenev M.Yu., Fyodorov V.B., Khrychev D.A., Khudak Yu.I., Shatina A.V. The image speed during the optical-electronic surfacing the planet. *Russ. Technol. J.* 2018;6(4):65–77 (in Russ.). <https://doi.org/10.32362/2500-316X-2018-6-4-65-77>

СПИСОК ЛИТЕРАТУРЫ

1. Геча В.Я., Жиленев М.Ю., Горчаков С.Ю., Новоселов С.А. Формулы расчета кинематических параметров орбитальной съемки планеты бортовой оптико-электронной аппаратурой космического аппарата. *Вопросы электромеханики. Труды ВНИИЭМ.* 2019;173(6):23–32. URL: <https://jurnal.vniem.ru/text/173/23-32.pdf>
2. Геча В.Я., Жиленев М.Ю., Федоров В.Б., Хрычев Д.А., Худак Ю.И., Шатина А.В. Скорость движения изображения при оптико-электронной съемки поверхности планеты. *Russian Technological Journal.* 2018;6(4): 65–77. <https://doi.org/10.32362/2500-316X-2018-6-4-65-77>
3. Жиленев М.Ю., Винтаев В.Н. Формула расчета движения изображения при орбитальной съемке планет оптико-электронной аппаратурой. *Телекоммуникации.* 2011;7:2–7.

3. Zhilenev M.Yu., Vintaev V.N. The formula for calculating the image motion during planet optoelectronic acquisition. *Telekommunikatsii = Telecommunications*. 2011;7:2–7 (in Russ.).
4. Brown E.B. V/H Image Motion in Aerial Cameras. *Photogramm. Eng.* 1965;31(2):308–323.
5. Gecha V.Y., Zhilenev M.Yu., Fedorov V.B., Khrychev D.A., Khudak Yu.I., Shatina A.V. Velocity field of image points in satellite imagery of planet's surface. *Russ. Technol. J.* 2020;8(1):97–109 (in Russ.). <https://doi.org/10.32362/2500-316X-2020-8-1-97-109>
6. Kawachi D.A. Image Motion and Its Compensation for the Oblique Frame Camera. *Photogramm. Eng.* 1965;31(1):154–165.
7. Gorchakov S.Yu. Synthesis of program angular motions of the Earth remote sensing spacecraft with high spatial resolution. *Russ. Technol. J.* 2021;9(3):78–87 (in Russ.). <https://doi.org/10.32362/2500-316X-2021-9-3-78-87>
8. Butyrin S.A. Kinematic synthesis of the spacecraft programmed attitude motion at the earth optic-electronic survey. *Izvestiya Samarskogo nauchnogo tsentra RAN = Izvestia of Samara Scientific Center of the Russian Academy of Sciences*. 200;9(3):664–670 (in Russ.). Available from URL: <https://cyberleninka.ru/article/n/kinematicheskiy-sintez-programmnogo-uglovogo-dvizheniya-kosmicheskogo-apparata-pri-optiko-elektronnoy-semke-zemli/viewer>
9. Mashtakov Ya., Tkachev S. Synthesis and constructing the angular motion of the remote sensing satellite for tracking the trajectory on the Earth surface. *Preprinty IPM im. M.V. Keldysha = Keldysh Institute Preprints*. 2014;20. 31 p. (in Russ.). Available from URL: <http://library.keldysh.ru/preprint.asp?id=2014-20>
10. Pavlis N.K., Holmes S.A., Kenyon S.C., Factor J.K. An Earth Gravitational Model to Degree 2160: EGM2008. *Geophysic. Res. Abstracts*. 10, EGU2008-A-01891, 2008, SRef ID: 1607-7962/gra/EGU2008-A-01891, EGU General Assembly.
11. Petit G., Luzum B. *IERS Conventions*. Frankfurt am Main, Germany: International Earth Rotation and Reference Systems Service; 2010. 179 p.
12. Canuto E., Massotti L., Montenegro C.P., Novara C., Carlucci D. *Spacecraft Dynamics and Control: The Embedded Model Control Approach*. Elsevier Ltd.; 2018. 779 p. <https://doi.org/10.1016/C2016-0-00420-5>
13. Bangert J., Bell S., Capitaine N. *SOFA Tools for Earth Attitude*. International Astronomical Union; 2021. 157 p.
14. Bangert J., Bell S., Capitaine N. *SOFA Time Scale and Calendar Tools*. International Astronomical Union; 2021. 67 p.
15. Urmaev M. *Kosmicheskaya fotogrammetriya (Space photogrammetry)*. Moscow: Nedra; 1989. 278 p. (in Russ.). ISBN 5-247-01273-9
4. Brown E.B. V/H Image Motion in Aerial Cameras. *Photogramm. Eng.* 1965;31(2):308–323.
5. Геча В.Я., Жиленев М.Ю., Федоров В.Б., Хрычев Д.А., Худак Ю.И., Шатина А.В. Поле скоростей движения точек изображения при орбитальной съемке поверхности планеты. *Russian Technological Journal*. 2020;8(1):97–109. <https://doi.org/10.32362/2500-316X-2020-8-1-97-109>
6. Kawachi D.A. Image Motion and Its Compensation for the Oblique Frame Camera. *Photogramm. Eng.* 1965;31(1):154–165.
7. Горчаков С.Ю. Синтез программных угловых движений космического аппарата дистанционного зондирования Земли с высоким пространственным разрешением. *Russian Technological Journal*. 2021;9(3):78–87. <https://doi.org/10.32362/2500-316X-2021-9-3-78-87>
8. Бутырин С.А. Кинематический синтез программного углового движения космического аппарата при оптико-электронной съемке Земли. *Известия Самарского научного центра РАН*. 2007;9(3):664–670. URL: <https://cyberleninka.ru/article/n/kinematicheskiy-sintez-programmnogo-uglovogo-dvizheniya-kosmicheskogo-apparata-pri-optiko-elektronnoy-semke-zemli/viewer>
9. Маштаков Я.В., Ткачев С.С. Построение углового движения спутника Д33 при отслеживании маршрутов на поверхности Земли. *Препринты ИПМ им. М.В. Келдыша*. 2014;20. 31 с. URL: <http://library.keldysh.ru/preprint.asp?id=2014-20>
10. Pavlis N.K., Holmes S.A., Kenyon S.C., Factor J.K. An Earth Gravitational Model to Degree 2160: EGM2008. *Geophysic. Res. Abstracts*. 10, EGU2008-A-01891, 2008, SRef ID: 1607-7962/gra/EGU2008-A-01891, EGU General Assembly.
11. Petit G., Luzum B. *IERS Conventions*. Frankfurt am Main, Germany: International Earth Rotation and Reference Systems Service; 2010. 179 p.
12. Canuto E., Massotti L., Montenegro C.P., Novara C., Carlucci D. *Spacecraft Dynamics and Control: The Embedded Model Control Approach*. Elsevier; 2018. 779 p. <https://doi.org/10.1016/C2016-0-00420-5>
13. Bangert J., Bell S., Capitaine N. *SOFA Tools for Earth Attitude*. International Astronomical Union; 2021. 157 p.
14. Bangert J., Bell S., Capitaine N. *SOFA Time Scale and Calendar Tools*. International Astronomical Union; 2021. 67 p.
15. Урмаев М. *Космическая фотограмметрия*. М.: Недра; 1989. 278 с. ISBN 5-247-01273-9

About the author

Sergei Yu. Gorchakov, Postgraduate Student, Higher Mathematics Department, Institute of Artificial Intelligence, MIREA – Russian Technological University (78, Vernadskogo pr., Moscow, 119454 Russia). E-mail: sygorchakov@yandex.ru. RSCI SPIN-code 2275-8579, <http://orcid.org/0000-0003-2266-5284>

Об авторе

Горчаков Сергей Юрьевич, аспирант, кафедра высшей математики Института искусственного интеллекта ФГБОУ ВО «МИРЭА – Российский технологический университет» (119454, Россия, Москва, пр-т Вернадского, д. 78). E-mail: sygorchakov@yandex.ru. SPIN-код РИНЦ 2275-8579, <http://orcid.org/0000-0003-2266-5284>

Translated from Russian into English by Kirill V. Nazarov

Edited for English language and spelling by Thomas A. Beavitt